JOURNAL OF MATERIALS SCIENCE **34** (1999) 3083–3093

Formation studies of TiC from carbon coated TiO_2

G. A. SWIFT, R. KOC
Department of Mechanical Engineering and Energy Processes, Southern Illinois University at Carbondale, Carbondale, IL 62901, USA
E-mail: swiftg@siu.edu, kocr@siu.edu

This paper deals with the formation of titanium carbide from carbon coated titanium dioxide precursors. This study makes use of differential scanning calorimetry (DSC), thermogravimetric analysis (TGA), X-ray diffraction (XRD), and both scanning and transmission electron microscopy (SEM and TEM). DSC curves of both coated and mixed 33.2 wt % carbon containing titania demonstrates the superiority of the coated precursor by exhibiting both more reactions and reactions at lower temperatures than the mixed powder. Weight loss as powders were reacted in argon at varying temperatures was measured using TGA, while heat flow vs. temperature was measured by DSC. The weight loss allowed for calculation of the activation energy of TiC via the formation of various lower oxides of titanium. The activation energy was calculated as 731.6 ± 24.2 kJ/mol. XRD was used to characterize the products resulting from the reaction of the carbon coated precursor at isotherms at each 100 °C interval from 1100 to 1500 °C, inclusive. These diffraction patterns support the hypothesis that the TiC formation proceeds through the formation of lower oxidation states of titanium.

1. Introduction

Most non-oxide ceramic materials have the advantages of high melting point, high strength even at high temperature, high wear resistance, low thermal expansion coefficient, and light weight. Metal carbides such as titanium carbide (TiC) are finding increased use as a result of excellent values for these properties.

The most common production method of ceramic parts is sintering. The starting materials for sintering are powders. The powders are raised to a temperature sufficient to cause mass transfer and densification. The starting powders must be of high quality with respect to five specific characteristics. The powders must be pure and single phase, have a narrow size distribution, be spherical in shape, be submicron in size, and be free of agglomerations. Failure in any of these criteria lessens the quality of the final sintered piece [1].

The most widely used process for TiC production is carbothermal reduction of titanium dioxide, TiO_2, in the presence of carbon, C. Carbothermal reduction produces large amounts of powder, and makes use of inexpensive precursor materials, however there is currently no commercial powder production process to produce TiC powder of submicron size [2].

The carbon coating process developed and patented by Koc and Glatzmaier has been applied to TiC powder production, and has produced TiC powder which meets all of the above criteria [2–4]. The same process has also been applied to TiN powder production. In order to demonstrate to industry the desirability of the coating process over conventional mixing processes, this study has been undertaken with the goal of determining the superiority of coated precursors to conventional mixed powders. Another consideration is the fact that TiC is a less expensive substitute for tungsten carbide, as WC requires cobalt as a binder for sintering, while TiC can use less expensive nickel as a binder [5].

The primary advantage provided by use of coated precursors is the intimate contact between reactants. Thermodynamic data makes no allowance for breaches in the contact between reactants, while in fact it will inhibit a reaction away from the ideal thermodynamic conditions. The intimate contact achieved with coated precursors allows the best possible chance for a reaction to proceed as per thermodynamic calculations. This advantage should also be evident as a result of this research.

The overall carbothermal reduction reaction to be studied is:

$$TiO_2 + 3C \rightarrow TiC + 2CO(g) \quad (1)$$

Reaction (1) proceeds thermodynamically at 1289 °C. The actual reaction series, however, most likely proceeds as the successive formation of lower oxides of titanium. The following possible reaction series, based upon Gibbs Free Energies (see Fig. 1), is proposed:

$$4TiO_2 + C \rightarrow Ti_4O_7 + CO(g) \quad (2)$$

$$3Ti_4O_7 + C \rightarrow 4Ti_3O_5 + CO(g) \quad (3)$$

$$Ti_3O_5 + 8C \rightarrow 3TiC + 5CO(g) \quad (4)$$

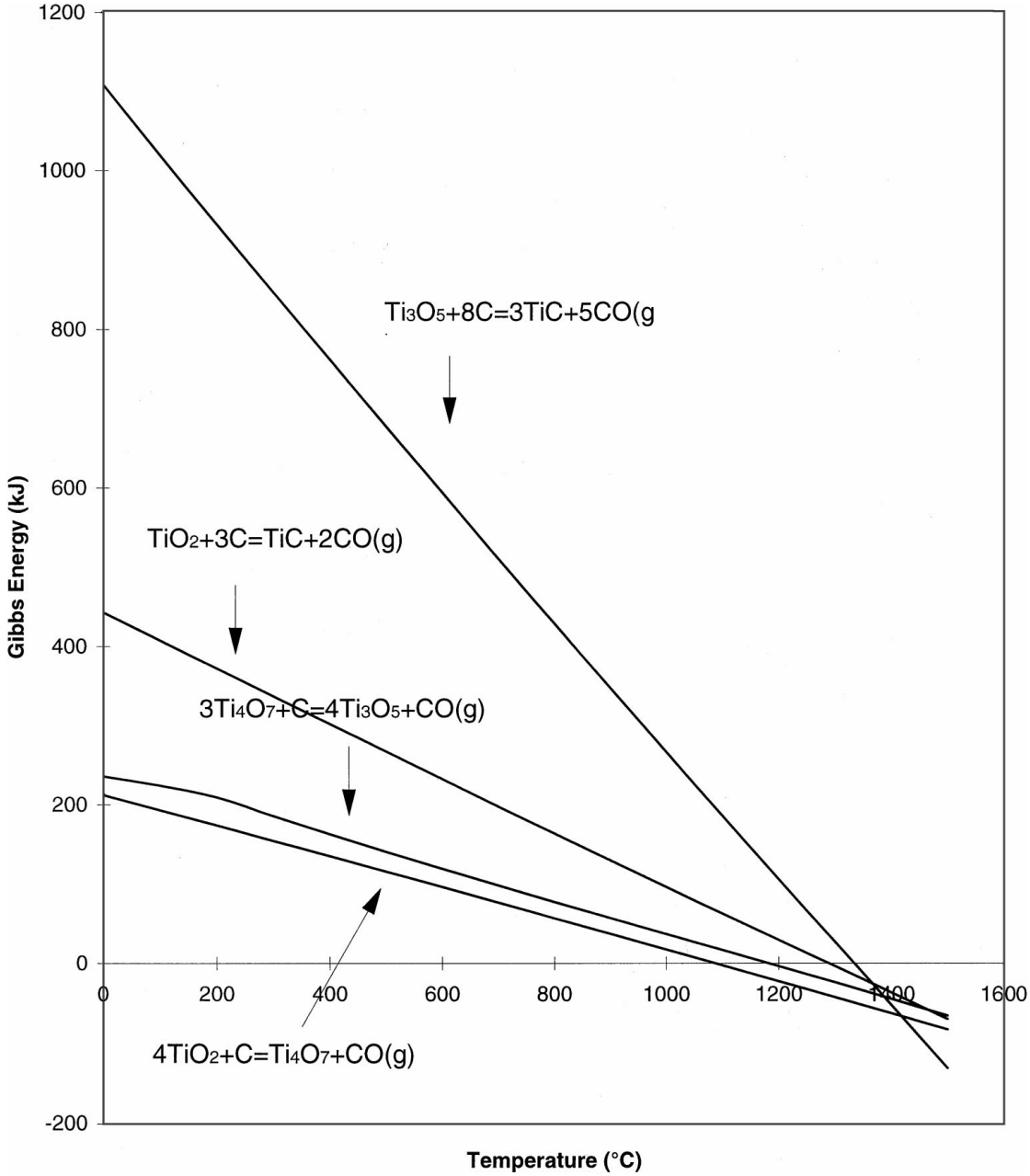

Figure 1 Gibbs free energy as a function of temperature for reactions (1–4).

Reactions (2), (3), and (4) occur thermodynamically at 1087, 1182, and 1334 °C, respectively. It is very likely that after reactions (2) and (3) occur, any as-yet unreacted TiO_2 will proceed at 1289 °C as per reaction (1) with Ti_3O_5 following reaction (4) once 1334 °C is reached.

The methods to be employed in this determination were Thermogravimetric Analysis (TGA), Differential Scanning Calorimetry (DSC), Transmission and Scanning Electron Microscopy (TEM and SEM), and X-ray Diffraction (XRD). The TGA data were used to determine the activation energy of the carbon coated TiO_2 in the formation of TiC. DSC data from both coated TiO_2 precursor and mixed powders showed the occurrence of reactions, with the sample exhibiting reaction(s) at lower temperature being superior. The products resulting from the reactions were characterized using TEM, SEM and XRD. Thermodynamic data and calculations were carried out using HSC Chemistry for Windows 3.0 (Outokumpu Research, Finland).

2. Experimental

2.1. Precursor preparation

First, the precursors were prepared. Both the mixed powder and coated precursor used submicron TiO_2 powder (P-25, Degussa Corp., Ridgefield Park, NJ), shown in Fig. 2, with surface area of 49.5 m^2/g. Note the relative state of agglomeration of the powders. Propylene gas (C_3H_6) was the source of carbon for the coated precursor, while carbon black (Monarch 880, Cabot, Waltham, MA) was used for the mixed powder.

The coated precursor was prepared by cracking C_3H_6 gas at 600 °C, with pyrolytic carbon coating the TiO_2. This process has been proven to be surface area activated, thus each TiO_2 particle is coated spherically

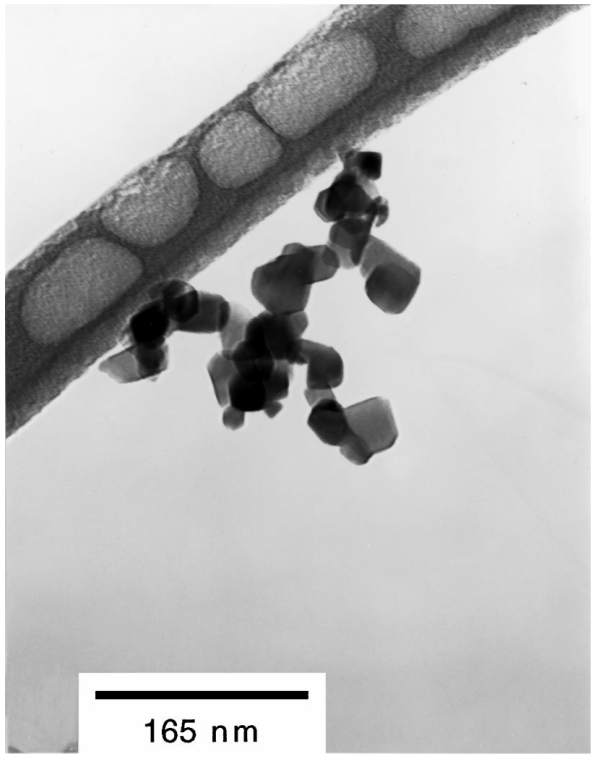

Figure 2 TEM micrograph of DeGussa P-25 TiO_2.

by a similar amount as every other (see Fig. 3). Coating was continued until the TiO_2 had been coated to 33.2 wt % C. The carbon coat is a porous, amorphous layer of carbon. The mixed powder was prepared in a plastic container, into which appropriate amounts of TiO_2 and carbon black were added to yield 33.2 wt % C. Two polymer balls were added to this mixture, and the container was placed in a Spex Mixer/Mill (Model 8000, Spex, Metuchen, NJ) for three mixing times of 20 min each.

2.2. DSC

After preparation of the precursor and mixed powder, a 15 mg sample of each was heated in a Pt crucible at 20 °C/min to 1500 °C in flowing argon in a Setaram Labsys TG-DTA/DSC (Setaram Corp., France). The heat flow as a function of temperature was recorded as DSC data, and is shown in Fig. 4. The curve for the mixed powder shows much less reaction than the coated precursor. In fact, the coated shows reactions at lower temperatures. The coated sample exhibits three clear endothermic reactions, each beginning at 1192, 1310, and 1389 °C. Each reaction proceeds at the completion of the previous reaction. The mixed sample shows reactions at 1354 and 1379 °C. This DSC data indicates that the coated sample experiences three complete reactions under 1400 °C, with initial reaction progression occurring at lower temperature than for the mixed.

2.3. TGA

In an effort to qualitatively determine the reaction products at the various stages of formation for the coated precursor, TGA was performed in the Labsys at 2 hour isotherms of 1100, 1200, 1300, 1400, and 1500 °C in a Pt crucible, with a heating rate of 20 °C/min in flowing argon. Each isotherm was performed three times. Each sample was weighed both before and after each experiment to measure the weight loss; these measured weight loss values were compared with the weight loss indicated by the Labsys. It was decided to attain less than 10% discrepancy between the measured weight loss of each sample and the weight loss as recorded by the software. The only exception to this was the data obtained from the 1400 and 1500 °C isotherms. The corrections applied to these data is explained later.

The TGA data was used to calculate the fraction converted, as shown in Fig. 5. (Note: fraction converted = wt % lost/theoretical wt % loss. From stoichiometry, the theoretical wt % loss was calculated as 48.33 wt % from Equation 1.) The fraction converted data was then used to calculate the activation energy according to the Arrhenius relation. Two methods were used to calculate the activation energy, in an attempt to guarantee accuracy.

3. Results and discussion

3.1. TGA

From the TGA data acquired, the fraction converted was calculated. For the isotherms of 1400 and 1500 °C corrections were made to the data before the curves shown were arrived at. The 1400 °C curves all exhibited a weight gain after the maximum weight loss was reached. The curve shown simply shows the extension of the maximum weight loss to the completion time. Since the weight loss occurred before this, the calculation of the reaction constant k is unaffected, as the weight loss slope is used for said calculation. For the 1500 °C curve, the software indicated a weight loss greater than the theoretical. Since the data was known to be erroneous by 8.25% from the measured value, the software weight loss was divided by the measured wt % loss. This yielded a value which was used as the initial powder weight, thus matching the software wt % loss to the measured wt % loss. All other data were multiplied by the same factor to present the curve shown.

For solid state material reactions, the weight loss is equal to the fraction of reaction completed, α, as assumed for these calculations. As noted above, two methods were used in computation of the activation energy. These methods are described below.

3.1.1. Method 1

It has been shown empirically that

$$\frac{d\alpha}{dt} = k^n t^{n-1}(1-\alpha) \tag{5}$$

applies to the isothermal kinetics of a variety of reactions, where t is time and k is the reaction rate constant [6]. If k and t are assumed independent of α, then

$$\ln \frac{1}{1-\alpha} = (kt)^n \tag{6}$$

$$\alpha = 1 - e^{-(kt)^n} \tag{7}$$

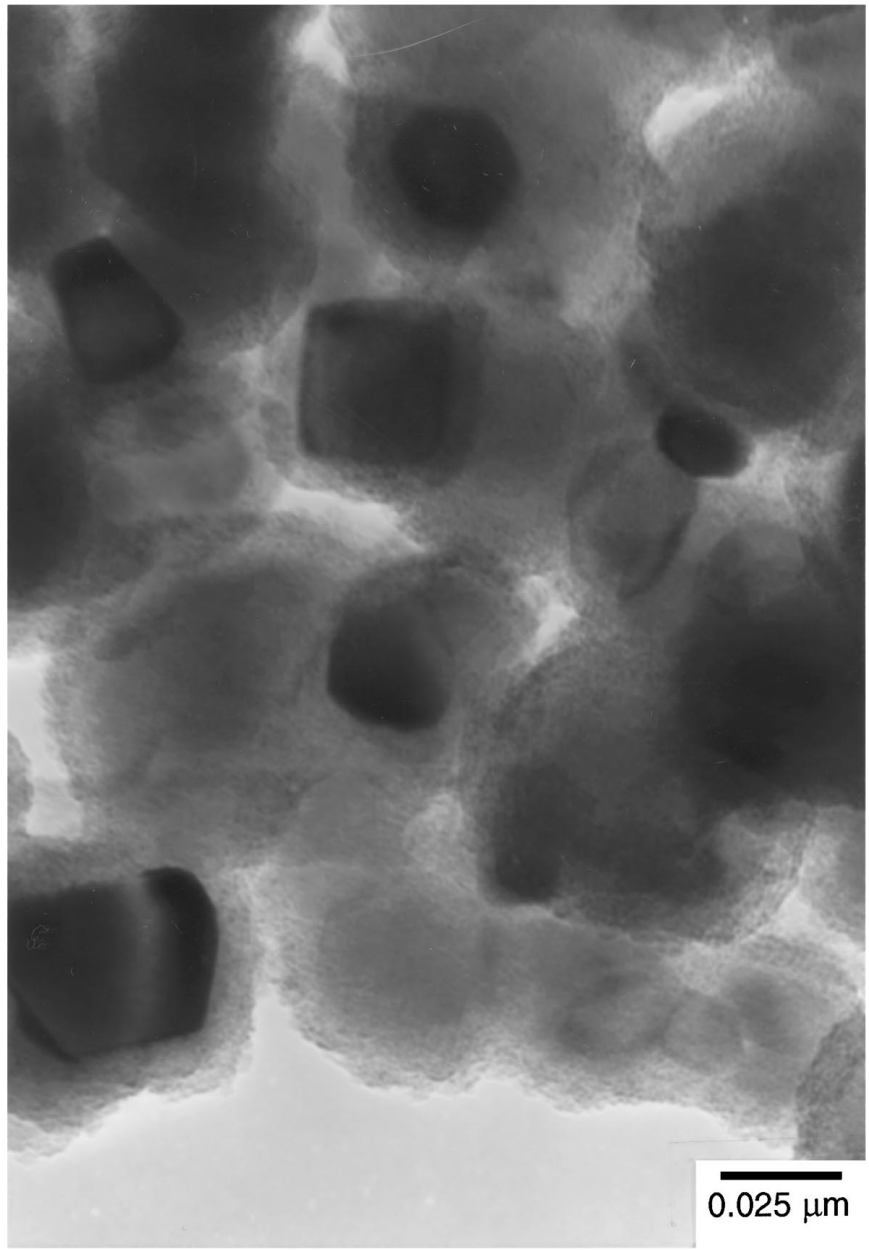

Figure 3 TEM micrograph of carbon coated DeGussa P-25 TiO_2 (Courtesy of Folmer).

[7, 8]. In order to calculate k, Equation 7 was transformed to:

$$\ln(1-\alpha) = -(kt)^n \tag{8}$$

and

$$\ln[-\ln(1-\alpha)] = n \ln k + n \ln t \tag{9}$$

When $\ln[-\ln(1-\alpha)]$ vs. $\ln t$ is plotted, the slope is n and the y-intercept is $n \ln k$. The slope and y-intercept apply to straight line fits of the fraction converted data. The results from these calculations are summarized in Table I.

TABLE I Ln k as a function of temperature using Method 1

Temperature (°C)	ln k
1100	−9.388
1200	−6.580
1300	−4.911
1400	1.320
1500	5.120

3.1.2. Method 2

For solid state reaction kinetics:

$$\frac{d\alpha}{dt} = k\alpha^n \tag{10}$$

It is generally assumed that the fraction of reaction completed is a function of time. The same was assumed for this method. The relation is of the form:

$$\alpha = f(t) \tag{11}$$

In the case when the α vs. t curve is linear, i.e. $\alpha = st + b$, the slope s is equal to the rate constant k. In this case, however, the curves were non-linear. Thus it was necessary to find the value of x for which the following

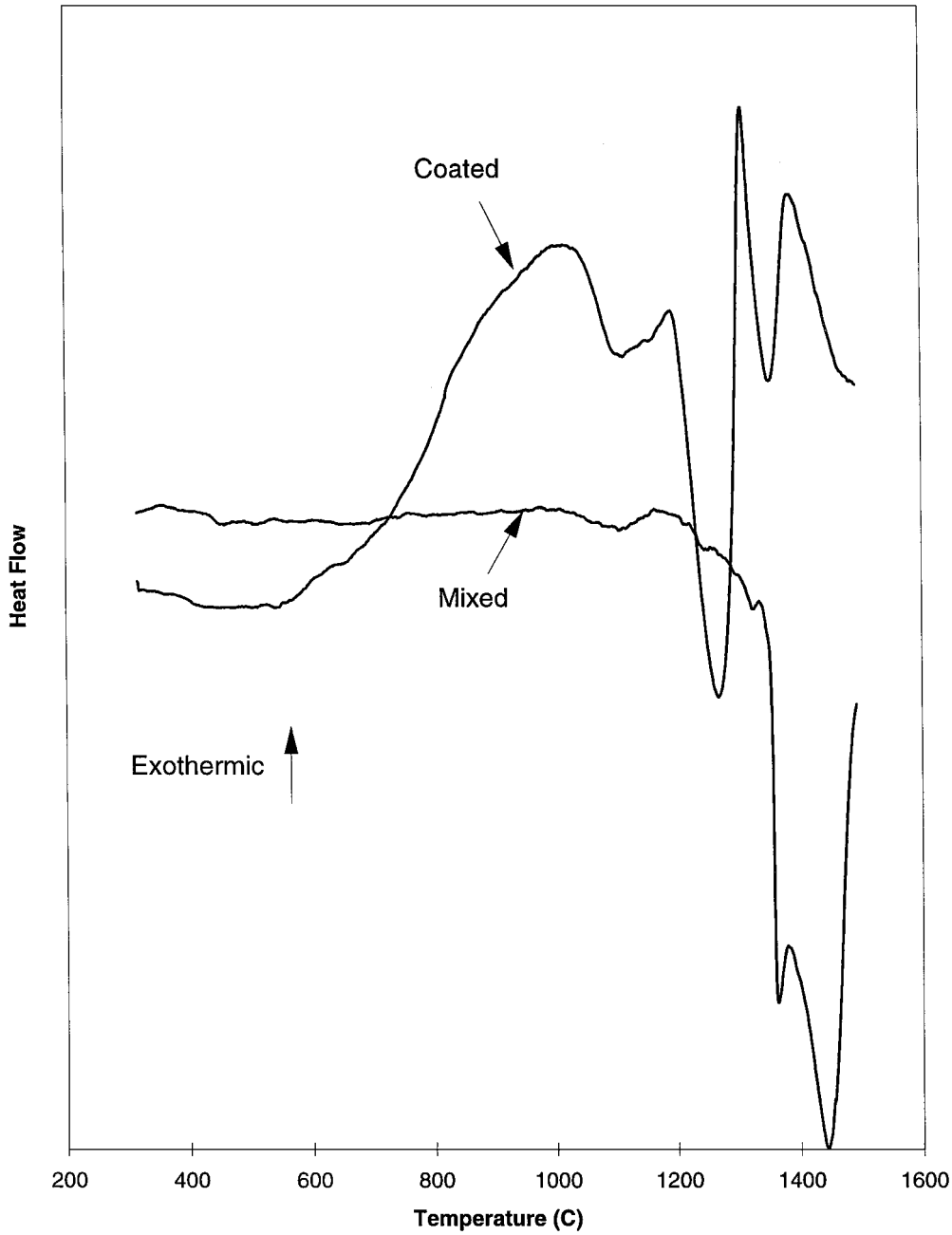

Figure 4 DSC curves for mixed and coated TiO_2-C. Samples were heated in a Pt crucible at 20 °C/min in flowing argon.

relation was linear:

$$\alpha = st^x + b \tag{12}$$

The solution to this required an iterative process attempting various x values for each isotherm's fraction converted data, until the most linear plot was achieved. After a good linear plot was achieved, further manipulation of Equation 12 was required to determine the value of k. The various transformations follow:

$$(\alpha - b)^{\frac{1}{x}} = s^{\frac{1}{x}} t \tag{12a}$$

$$\frac{1}{x}(\alpha - b)^{\frac{x-1}{x}} \frac{\mathrm{d}\alpha}{\mathrm{d}t} = s^{\frac{1}{x}} \tag{12b}$$

$$\frac{\mathrm{d}\alpha}{\mathrm{d}t} = \left(xs^{\frac{1}{x}}\right)(\alpha - b)^{\frac{x}{x-1}} \tag{13}$$

Equation 13 is of the form of Equation 10. Thus from Equation 13, $k = xs^{1/x}$. The results of these calculations are presented in Table II.

3.1.3. Activation energy

Using the data obtained for ln k from both Method 1 and Method 2, the activation energy was calculated. Plots of ln k vs. t were prepared, and a straight line fit was applied to both data sets. According to the Arrhenius relation:

$$k = Ae^{-\frac{E}{RT}} \tag{14}$$

Transformation of Equation 14 yields:

$$\ln k = \ln A - \frac{E}{RT} \tag{15}$$

Equation 15 is of the form, $y = mx + b$, with slope $m = -\frac{E}{R}$, $x = \frac{1}{T}$, and $b = \ln A$. Thus by plotting $\ln k$ (from both Method 1 and Method 2) vs. $\frac{1}{T}$, the slope is equal to the activation energy, E, divided by the Universal Gas Constant, R. Fig. 6 shows $\ln k$ plotted vs. $1000/T$. Using $R = 8.314$ J/mol K, with slope values for Method 1 and Method 2 equal to $-88{,}000$ and $-99{,}106$ K, respectively, the activation energies were calculated. Method 1 had $E = 731.6 \pm 24.2$ kJ/mol, while Method 2 had $E = 824.0 \pm 32.4$ kJ/mol. These results are not especially different, so it can be assumed that the values are sufficiently accurate since two separate methods were kJ/mol used to arrive at each result.

TABLE II Ln k as a function of temperature using Method 2

Temperature (°C)	ln k
1100	−10.959
1200	−6.029
1300	−5.869
1400	1.425
1500	5.931

Linear regression was used to fit the straight lines to these data, therefore it was possible to calculate the accuracy of the fit to the data. The closer to 1 for the value of R^2, the better the fit. Method 1 had $R^2 = 0.9338$, while method 2 had $R^2 = 0.9213$. From this, Method 1 has the better accuracy to the data, and should be considered better data than Method 2.

3.2. XRD

XRD was performed on products resulting from each isotherm (Model DMAX-B, Rigaku, Tokyo, Japan).

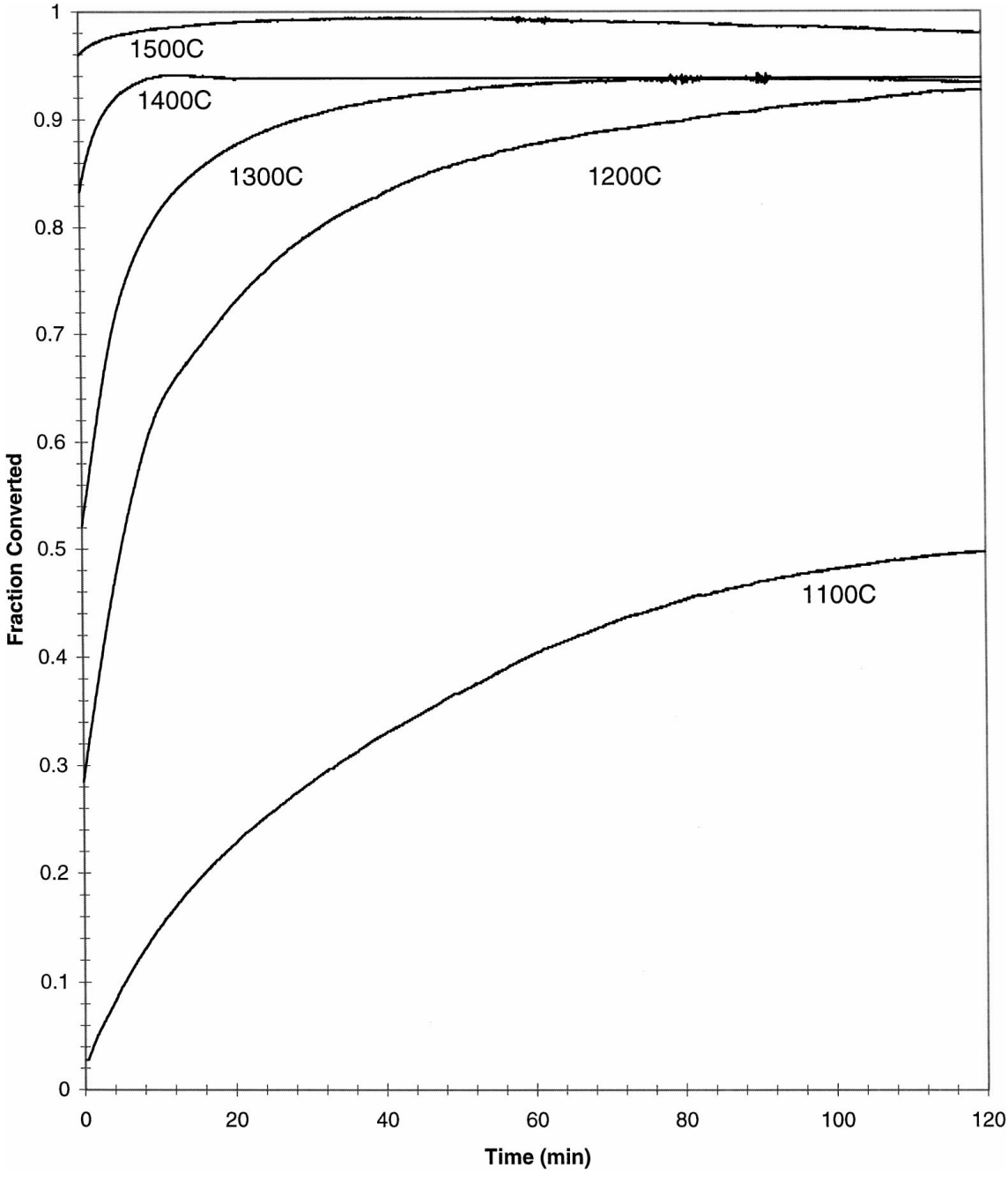

Figure 5 Fraction converted as a function of time for carbon coated TiO_2, at varying reaction temperatures.

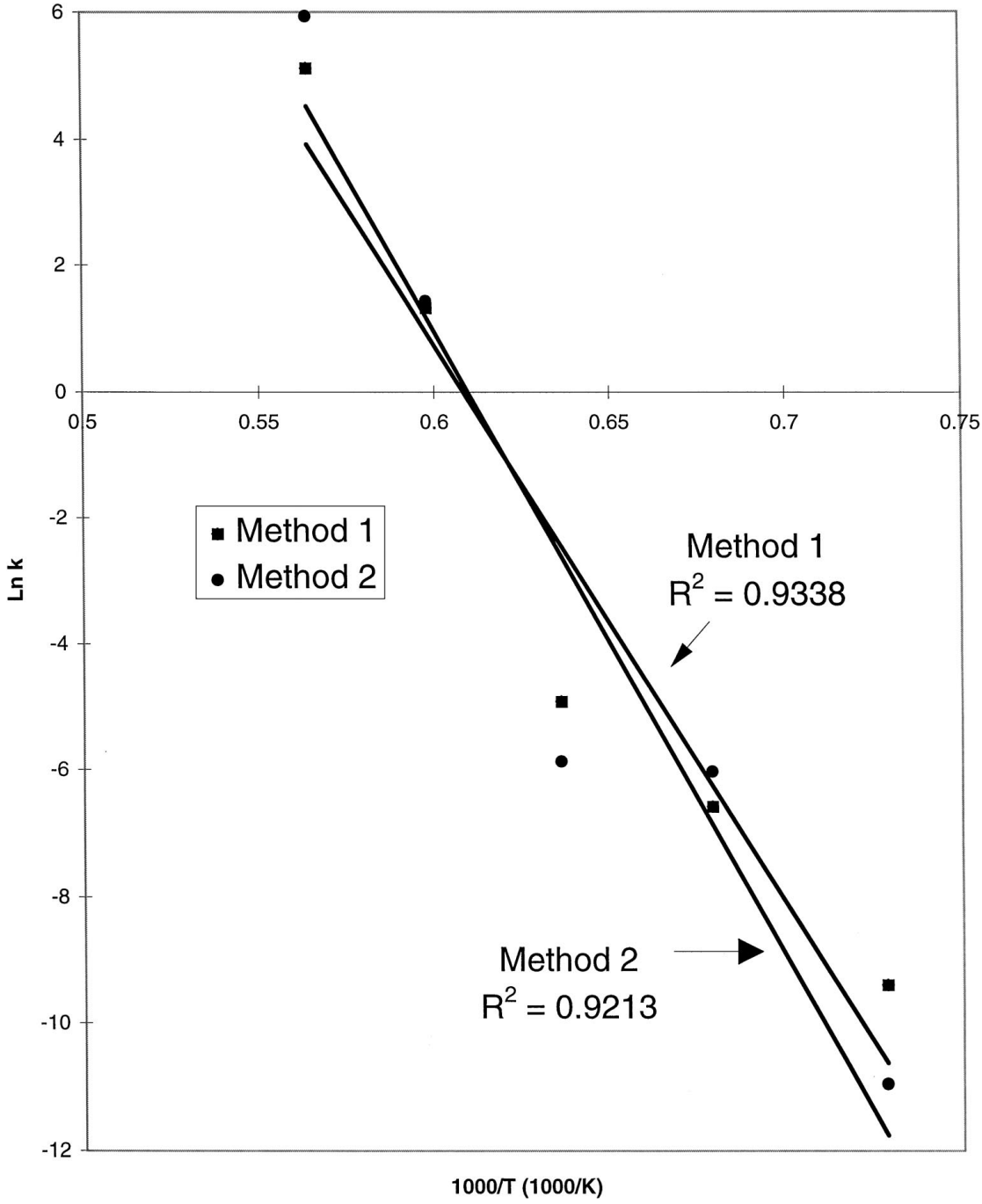

Figure 6 ln k vs. $1000/T$ for methods 1 and 2.

The diffraction patterns resulting are shown in Fig. 7. Each peak has a label serving as identification for the compound most likely to cause a peak at that 2-theta measure. The identification of compounds used JCPDF card files to match peak positions of possible oxides of titanium, titanium oxycarbide (TiC_xO_y), and titanium carbide. The cards used for each compound were: TiO_2 = 21-1272, Ti_4O_7 = 18-1402, Ti_3O_5 = 09-0309, TiO = 23-1078, and TiC = 32-1382. Other phases present are unknown; thus there may be some of the Magneli Phases.

At 1100 °C, the XRD pattern indicates very little in the way of TiC formation. There are only two TiC_xO_y peaks in evidence. There are two peaks for Ti_4O_7, which supports the earlier proposed reaction sequence. There are also several peaks which correspond to both TiO and Ti_3O_5. Previous research has indicated that TiO is present in solid solution as the TiC reaction progresses [9, 10]. Thermodynamically, however, the reaction

$$TiO_2 + C \rightarrow TiO + CO(g) \qquad (16)$$

does not proceed until 1393.4 °C. Thus it is more likely that the phase which generated the peaks is Ti_3O_5 or some unknown Ti_xO_y phase. Whichever is the case, the possibility that the phase is TiO seems very unlikely, when the thermodynamic reaction temperature is less than that of the titanium oxides suggested in the reaction sequence. Also are present several clearly Ti_3O_5 peaks; this would seem a good correlation to the previous statement. It is also important to note that very few TiO_2

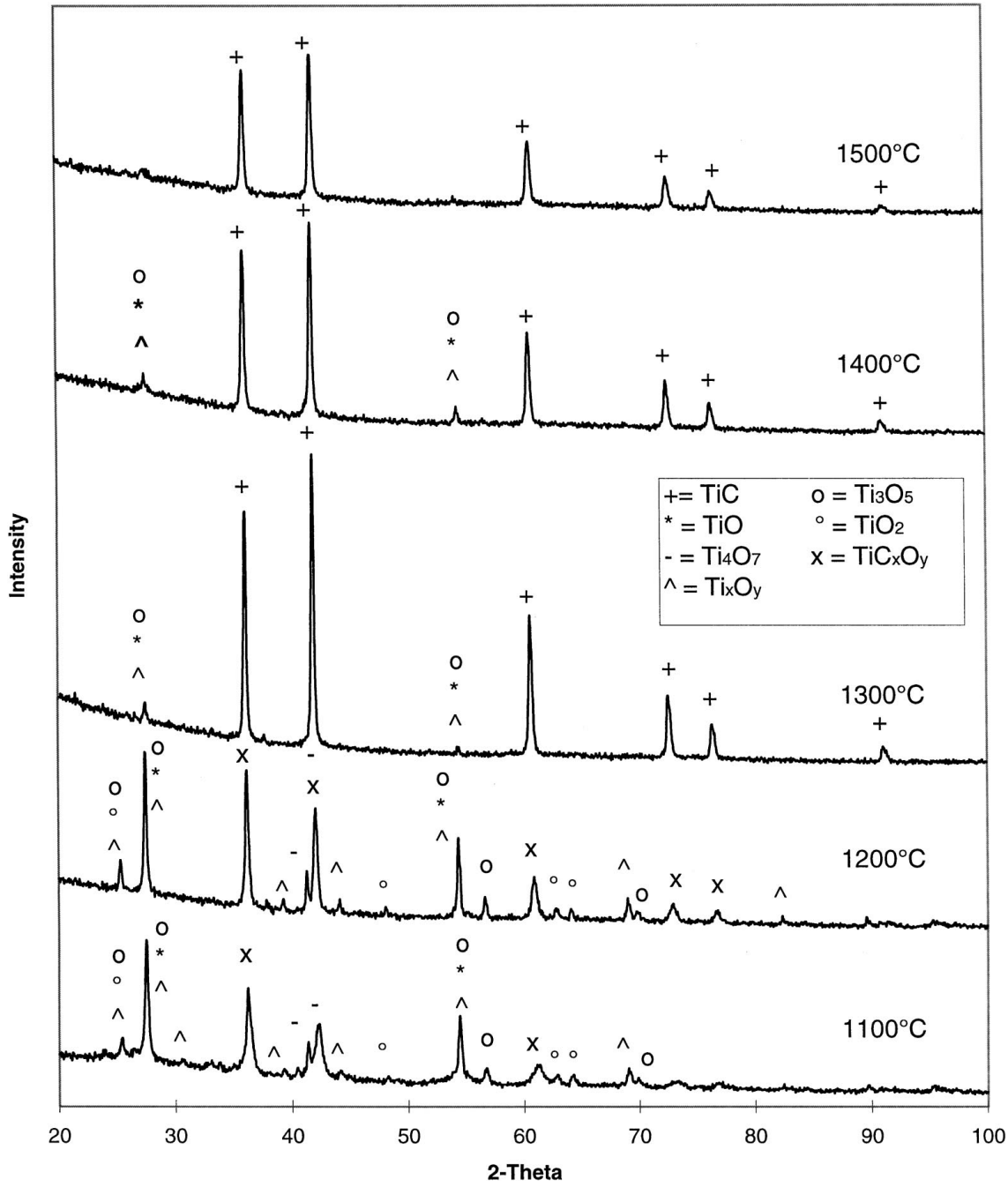

Figure 7 XRD patterns for carbon coated TiO_2, at varying reaction temperatures.

peaks are present. Since few peaks are evident, it is clear that the reduction process is already well under way.

The 1200 °C pattern shows appears much the same as the 1100 °C pattern. The differences are the increased amplitude of the TiC_xO_y peaks, as the powder is reduced further due to the higher temperature. Also, the Ti_4O_7 peaks have decreased in amplitude. In fact, one peak seems to be changing from Ti_4O_7 into TiC_xO_y. The peak has moved slightly left from the 1100 °C peak, but not so far as to coincide with the obviously TiC peak in the higher temperature patterns. Also are present the peaks of Ti_3O_5 or Ti_xO_y which coincide with the position of peaks from TiO patterns.

At 1300 and 1400 °C, TiC is the most prevalent compound, as indicated by the decreased broadness and increased amplitude of the peaks. There are, however, the remnants of two titanium oxide peaks which each occur at 2-theta measures consistent with both TiO and Ti_3O_5. It is not certain whether these peaks belong to one of these two compounds or to an unknown Ti_xO_y phase. As explained earlier, however, the peaks are most likely those of Ti_3O_5. At 1500 °C, TiC is the only remaining product of sufficient quantity to cause diffraction peaks. All TiC_xO_y and Ti_xO_y peaks have been eliminated.

Note the decreasing intensity of the peaks at 1400 and 1500 °C from the intensity at 1300 °C. It is known that a decrease in peak intensity can be caused by increased grain size of the analyzed powder [11]. Thus it was postulated that this decrease was due to the sintering of the powder at the higher reaction temperatures, as sintering would cause grain coarsening and growth in the powder sample.

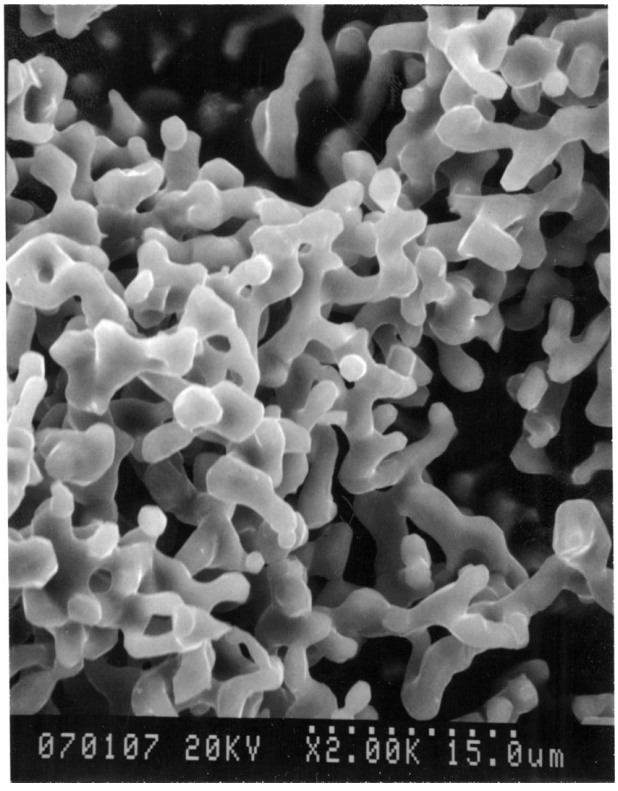

Figure 8 SEM micrograph of carbon coated TiO_2 reacted in a Pt crucible at 1500 °C for 2 h in flowing argon.

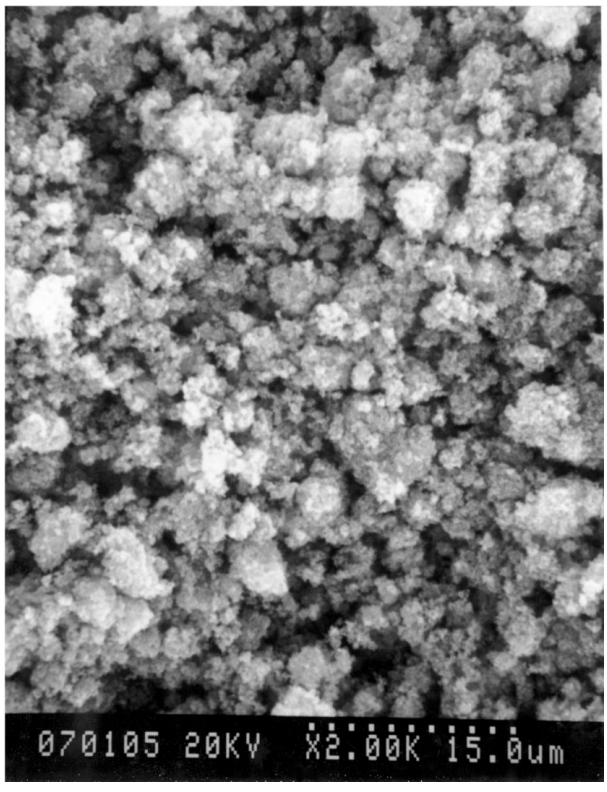

Figure 9 SEM micrograph of carbon coated TiO_2 reacted in a Pt crucible at 1300 °C for 2 h in flowing argon.

3.3. Electron microscopy

The powder resulting from the 1500 °C runs with the coated precursor were examined using SEM (Hitachi S570, Hitachi, Japan), as seen in Fig. 8. From the micrograph, it is clearly seen that the powders have been agglomerated (probably neck growth). An examination of the powders from 1300 °C, Fig. 9, shows none of this. The 1300 °C product also has much smaller particles.

The mechanism of this agglomeration can be the result of two conditions, or a combination of both. First, the high heating rate may not allow complete conversion of one or more lower oxides of titanium. If a phase with a melting temperature lower than the reaction temperature was not completely eliminated, its melting could cause sintering of particles. Or the reaction system could be the cause. The disk type TG-DSC of the Labsys does not allow the argon to flow directly over the powder as it might in a tube furnace, thus removal of all product gases might not be possible. This could allow lower oxides to re-form prior to final TiC formation with a result similar to the previous case.

Previous work has shown that this process produces superior TiC powders [3]. Fig. 10 (courtesy of Kodambaka) shows powder produced in a tube furnace with a lower heating rate and longer reaction time than used for the TGA of this paper. This powder resulted from an initial precursor carbon content of 32.6 wt % C. It is necessary to note that the analytical method of TGA is used primarily as a kinetic analysis, not for product characterization. The use of high heating rates, unattainable for large-scale industrial batch production, affects the resulting products, but is crucial for determining reaction characteristics.

4. Conclusion

This research has proven, through the use of various analytical methods including TGA, DSC, and XRD, that the formation of TiC by carbothermal reduction of carbon coated TiO_2 proceeds through the formation of lower oxides of titanium. The process first forms Ti_4O_7, then Ti_3O_5, with unknown TiC_xO_y and Ti_xO_y phases forming simultaneously. The reaction is essentially completed at 1300 °C, with higher temperatures providing the final purification into TiC. The activation energy for the formation of TiC using the carbon coated precursor is 731.6 kJ/mol.

The sintering of TiC produced by this process with Ni has been investigated in detail by Meng, with results presented as a poster at the 1997 ACerS conference in Cincinnati, OH, and soon to be published. Nickel powder and the as-produced TiC were wet-milled in ethyl alcohol in a WC container for 2 hours. The same was done for H.C. Starck TiC. Compaction resulted in a green density of ~60% of theoretical density. Figs 11 and 12 (courtesy of Meng) show the SEM images of the TiC-Ni sintered in a tube furnace at 1500 °C for 2 hours in flowing 10%H_2-Ar atmosphere. The images shown are from sintered pellets with 10 wt % Ni; note that TiC powder produced via the coating method has been sintered with 3 wt % Ni, while industry generally uses 20 wt %. Fig. 11 shows much less porosity than Fig. 12. As porosity in the final sintered piece is detrimental to properties such as strength and conductivity, the commercially available Starck powder is clearly inferior to that produced using the coating method.

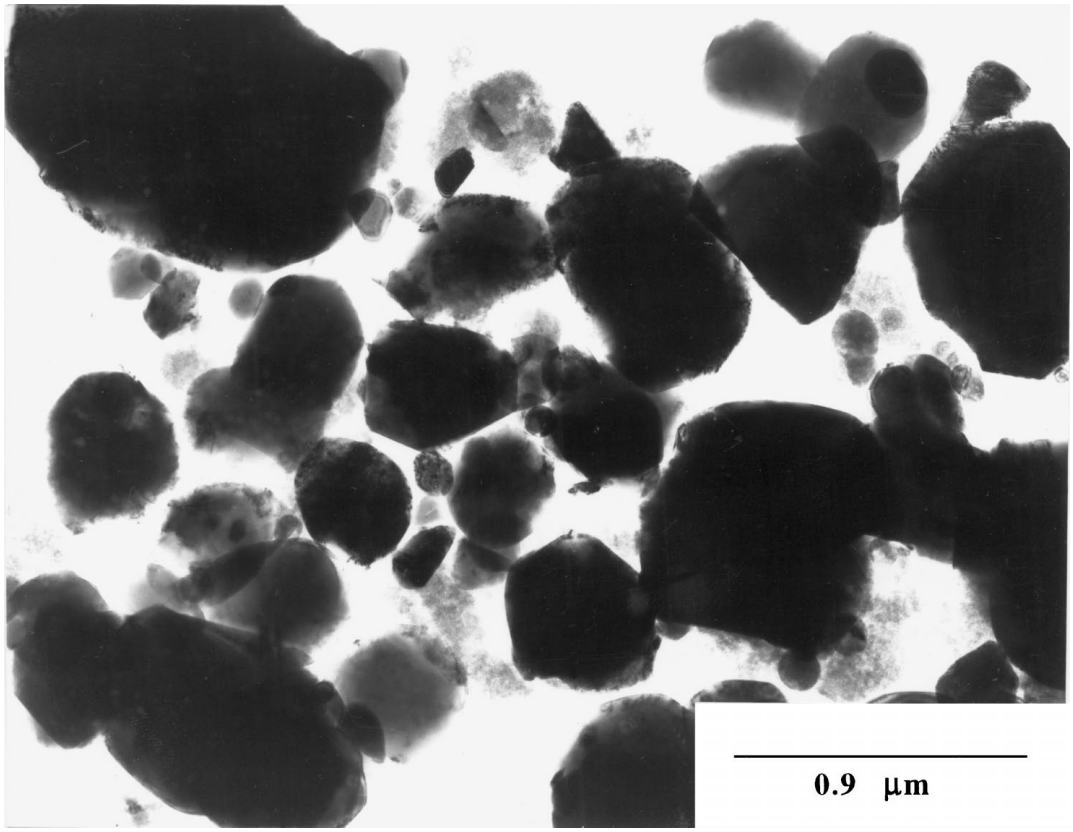

Figure 10 TEM micrograph of TiC powder produced in a tube furnace from carbon coated TiO_2 reacted 4 h at 1550 °C in a graphite boat, with a 7 °C/min heating rate, milled 2 h in a WC container (Courtesy of Kodambaka).

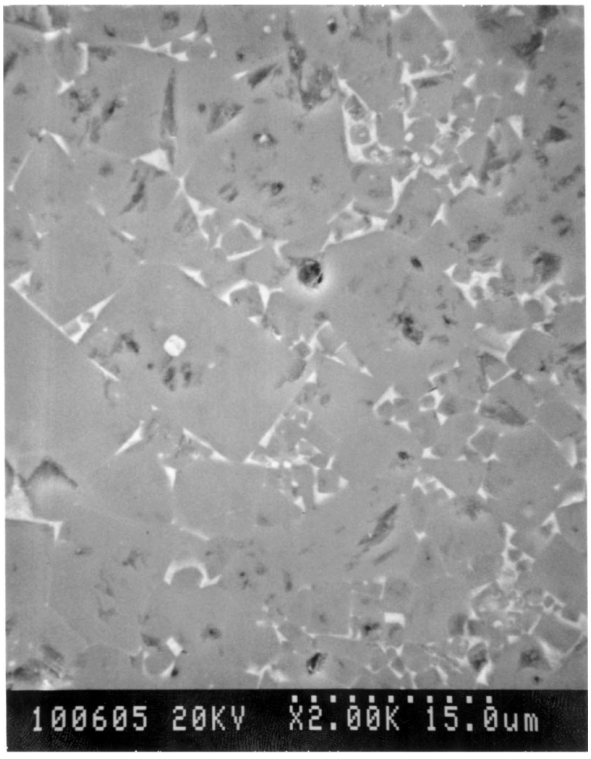

Figure 11 SEM micrograph of polished surface of sintered TiC-10 wt % Ni, produced from TiC from the coating method, sintered at 1500 °C for 2 h in flowing 10%H_2-Ar (Courtesy of Meng).

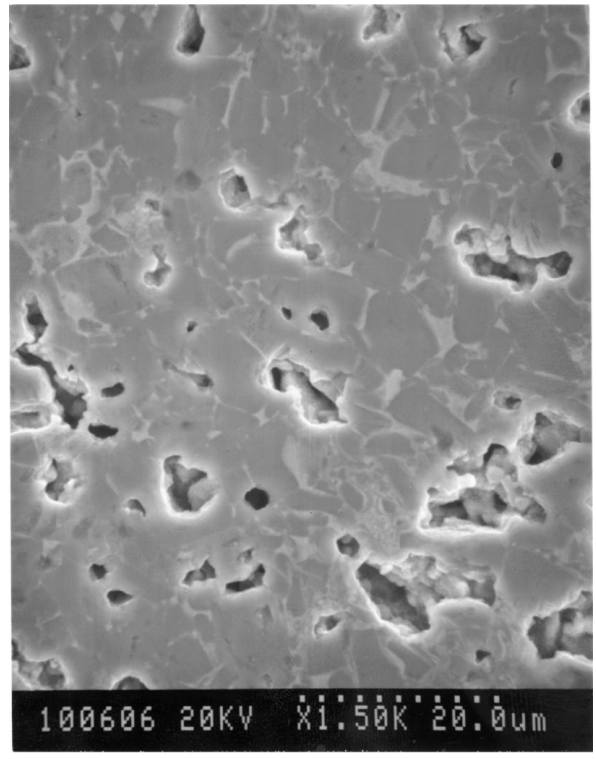

Figure 12 SEM micrograph of polished surface of sintered TiC-10 wt % Ni, produced from H. C. Starck TiC, sintered at 1500 °C for 2 h in flowing 10%H_2-Ar (Courtesy of Meng).

Acknowledgements

The authors would like to thank Dr. Charles Sorrell for his continuing interest in this work. For TEM and SEM micrographs as noted, the authors thank Jeffrey Folmer, Chang Meng, and Suneel Kodambaka. The authors would also like to thank Gerald Fink for XRD assistance, and the Center for Electron Microscopy at SIUC for their time and patience.

This research was sponsored by the U.S. Department of Energy, Office of Industrial Technologies, as part

of the Advanced Industrial Materials Program, under contract DE-AC05-84OR21400 with Lockheed Martin Energy Systems, Inc.

References

1. M. N. RAHAMAN, "Ceramic Processing and Sintering" (Marcel Dekker, Inc., New York, 1995).
2. R. KOC and G. GLATZMAIER, "Process for Synthesizing Titanium Carbide, Titanium Nitride, and Titanium Carbonitride," US Patent no. 5,417.952 (1995).
3. J. FOLMER, Master Thesis from Southern Illinois University at Carbondale, "Synthesis of Titanium Carbide Using Carbon Coated Titanium Dioxide Precursors," 1996.
4. G. GLATZMAIER and R. KOC, "Method for Silicon Carbide Production by Reacting Silica with Hydrogen Gas," US Patent no. 5,342.494 (1994).
5. P. ETTMAYER, *Annu. Rev. Mater. Sci.* (1989) 145–164.
6. J. BURKE, "The Kinetics of Phase Transformations in Metals" (Pergamon Press, London, 1965) pp. 50.
7. W. F. JOHNSON and R. F. MEHL, *Trans. AIME* **135** (1939) 416.
8. M. AVRAMI, *J. Chem. Phys.* **7**(12) 1103–1112.
9. L. M. BERGER, *J. Hard Metals* **3**(1) (1992) 3–15.
10. R. KOC, *J. Euro. Cer. Soc.* (1997) 1309–1315.
11. B. D. CULLITY, "Elements of X-Ray Diffraction," 2nd ed. (Addison-Wesley Publishing Company, Inc., London, 1978).

Received 31 July 1998
and accepted 27 January 1999